Airburst Modeling

Mark Boslough

Contents

Abstract

Computational models are used to gain insight about the phenomena associated with airbursts caused by the hypervelocity entry, ablation, breakup, and explosion of asteroids and comets in planetary atmospheres. Among the resulting discoveries has been the recognition that airbursts caused by downwardly directed collisions do more damage at the surface than a nuclear explosion of the same yield. They are therefore more dangerous than previously thought. At Sandia National Laboratories, the multidimensional, multi-material shock-physics code, CTH, has been run on high-performance computers using adaptive mesh refinement to resolve phenomena across spatial scales over many orders of magnitude. These simulations have led to the discovery of unexpected phenomena that emerge from the highly directed geometry of these events, such as ballistic plumes that rise to low Earth orbital altitudes before collapsing, ring vortices that descend to the surface and add to the list of damage mechanisms, and the splitting of shallow entry wakes into linear vortices that become visible as twin condensation trails.

M. Boslough (✉)
Sandia National Laboratories, Albuquerque, NM, USA
e-mail: mbboslo@sandia.gov

J.N. Pelton, F. Allahdadi (eds.), *Handbook of Cosmic Hazards and Planetary Defense*,
DOI 10.1007/978-3-319-03952-7_56

As scientific understanding has improved, these models are ready to be focused on systematic, high-fidelity, multiscale, multi-physics-based quantitative risk assessments to objectively inform policy decisions associated with planetary defense.

Keywords
Airburst • Airburst altitude • Asteroid • Comet • Eulerian shock-physics code CTH – Fireball • Impact • Pancake model – Shockwave • Thermal Radiation – Type 1 and Type 2 Airburst • Tunguska • Chelyabinsk • NEO • Libyan Desert Glass • Equivalent megatons • Shoemaker-Levy 9 (SL9) • FEMA

Introduction

When an asteroid (or comet) enters a planetary atmosphere at cosmic velocity, extremely high aerodynamic forces cause it to decelerate. The hypervelocity object also produces a strong shock wave as it passes through the atmosphere. Directly in front of it, at the apex of the bow shock, the atmosphere is compressed, heated, and ionized. Plasma temperatures can reach 25,000–30,000 K. The hot, opaque cap of plasma emits an enormous flux of thermal radiation that is absorbed by the leading surface of the impactor, causing rapid vaporization and ablation. If the body is small it completely ablates, leaving only a trail of ionized air and meteoritic vapor. If it is very large, it reaches the ground intact before a significant fraction of its mass can ablate and still moving at hypervelocity. It forms an impact crater.

This chapter describes what happens to objects with sizes between these two bounding cases, when they are "just right" (a condition that depends on many factors, including speed, density, strength, shape, and entry angle). As a body in this size range continues to descend through the atmosphere, it moves up the exponential density gradient faster than it slows down. Dynamic pressure increases rapidly until it exceeds the material strength of the body, causing it to deform and fragment. Both of these processes cause the cross-sectional area-to-volume ratio to increase. As the deforming and fragmenting object continues to encounter the steep density gradient, the stopping force, deceleration, and ablation can increase abruptly, eventually reaching a threshold in which it is better described as a multiphase, turbulent fluid consisting of fragments in a high-temperature plasma bath. Under these conditions, the radiative transfer of energy from the plasma to the fragments is on a timescale that is much faster than the resulting vapor can expand, and the internal pressure rises abruptly. It is possibly boosted by internally generated shock waves, leading to a type of nonchemical "detonation." The end result is an explosion as the high-pressure mixture of air and meteoritic vapor expands outward against its lower-pressure surroundings. This explosion is called an "airburst." This term originally applied to explosive weapons, including nuclear devices. According to Glasstone and Dolan (1977), "Provided the nuclear explosion takes place at an altitude where there is still an appreciable atmosphere, e.g., below about 100,000 ft, the weapon residues almost immediately incorporate material from the surrounding medium and form an intensely hot and luminous mass, roughly spherical in shape, called the 'fireball.'

An 'air burst' is defined as one in which the weapon is exploded in the air at an altitude below 100,000 ft, but at such a height that the fireball (at roughly maximum brilliance in its later stages) does not touch the surface of the earth."

The details in the above description of a nonnuclear collisional airburst have never been adequately modeled. Zahnle (1992) and Chyba et al. (1993) developed a much simplified semi-analytical model that combined parameterized equations for aerodynamic drag, heat transport and ablation, and a continuum deformation model for the impactor. The resulting "pancake model" is described by a set of coupled differential equations for each of these processes:

$$m\frac{dv}{dt} = -\frac{1}{2}C_D\rho A v^2 \tag{1}$$

$$q\frac{dm}{dt} = -\frac{1}{2}C_H\rho A v^3 \tag{2}$$

$$r\frac{d^2r}{dt^2} = -\frac{1}{2}C_D\frac{\rho}{\rho_m}v^2 \tag{3}$$

where m, v, A, q, and ρ_m are the instantaneous mass, velocity, cross-sectional area, heat of ablation, and density of a projectile, respectively, and ρ is the atmospheric density (which increases exponentially with decreasing altitude). C_D and C_H are the drag and heat transfer coefficient, respectively.

It is immediately obvious that this model neglects the detailed physical processes that take place on scales smaller than the asteroid itself. Whereas it is useful for estimating the energy conversion rate and determining altitude of maximum energy deposition for various assumptions, it ignores the actual means by which the conversion takes place. In this sense it is analogous to thermochemical models of explosive detonation, which do a good job at the macroscale and are useful for quantitative calculations of detonation effects such as launching plates or generating air blasts, but do not describe the meso- or microscale process of the detonation itself (shear heating, pore collapse, grain-boundary interactions, chemical kinetics, etc.).

Little progress has been made on such a multiscale approach to airburst modeling, but the development of high-resolution, multi-material, multidimensional hydrocodes such as CTH have made it possible to advance the state of macroscopic airburst modeling far beyond the pancake model. These computational hydrodynamic models – which are focused primarily on determining airburst effects and explaining airburst phenomenology rather than the modeling the multiscale airburst process itself – are the subject of this chapter.

Airburst Description

A large amount of energy is coupled directly to the Earth's atmosphere from hypervelocity collisions. Impacts are increasingly recognized both as a geologic process and as a human hazard. The atmosphere plays an important role even for

many crater-forming impacts. Melosh and Collins (2005) showed that the iron projectile that formed Meteor Crater (Arizona) deposited as much as 2.5 times more energy directly into the atmosphere than it carried to the surface. The projectile was estimated to have 9.0 Mt of kinetic energy at the top of the atmosphere and only 2.5 Mt when it struck the surface (megatons are the units often used to quantify the kinetic yield of planetary impacts; one megaton is 4.184×10^{15} J). Even more energy would have been added to the atmosphere from the surface explosion and hypervelocity debris that is ejected from the surface impact (Schultz 1992).

Much scientific understanding of airbursts was derived from models of the 1994 collision of Comet Shoemaker-Levy 9 (SL9) with Jupiter. Jupiter is a gas giant with no solid surface, so there was no "impact" in the conventional sense. With a relative velocity of 60 km/s, the specific kinetic energy density of each fragment was about 2×10^9 J/kg. The equivalent of a ton of TNT worth of kinetic energy was therefore carried into the Jovian atmosphere by every 2 kg of the comet. When each of the twenty or so fragments reached a depth where the density was sufficiently high for the aerodynamic pressure to exceed the strength of the material, it experienced catastrophic breakup which caused an exponentially reinforcing feedback between the radial expansion and fragmentation (which increases drag) and dynamic pressure (which drives those processes). As the fragments plunged into the dense part of the atmosphere, they experienced strain rates approaching those associated with a hypervelocity impact onto a solid surface. The rate of conversion from kinetic to internal energy was comparable to (or greater than) chemical energy release from a high explosive, resulting in an event that was indistinguishable from a detonation. The observed phenomena associated with SL9 demonstrated the enormous destructive potential of airbursts from exploding comets or asteroids and stimulated more research on analogous events in Earth's atmosphere.

The vast majority of meter and ten-meter-scale objects that collide with the Earth exhibit behavior somewhat like the fragments of SL9 – they fail to reach the ground intact because they are too small. About 50 meteoroids with diameters larger than 10 cm enter the atmosphere every day (Brown et al. 2002). A few of these break up into fragments that are strong enough to be decelerated without exploding and survive to strike the surface at low velocity as meteorites. Objects larger than about 2 m enter the atmosphere several times per year. Most of these completely disintegrate in the upper atmosphere, generating a high-altitude airburst with an explosive energy exceeding about 1 kt. Only asteroids larger than 20 m or so in diameter are capable to penetrating at hypervelocity into the lower atmosphere (the lower stratosphere or troposphere), where they generate megaton-scale explosions. It is uncertain how often such an event takes place, but estimates range from every few decades to less than one per century. Such an explosion could cause property damage or loss of life if it occurred over a populated area, but the greatest associated hazard might be that it could be misinterpreted as an act of aggression, potentially leading to a dangerous response.

The 1908 Tunguska event in Siberia is the only clear example of a low-altitude burst witnessed in modern times, with kinetic yield in excess of a megaton. Until the 2013 airburst over Chelyabinsk, Russia, it provided the only anchor point for

assessments of the impact hazard and only an indirect benchmark by which to compare models. Estimates of the Tunguska magnitude have varied widely, from a high value of about 700 Mt (Turco et al. 1982) to a low value of 3–5 Mt (Boslough and Crawford 1997). A widely quoted magnitude range has been between 10 Mt and 40 Mt (Vasilyev 1998) based on historic barograms, seismic records, and forest damage. These yield estimates were derived by comparing data from the Tunguska event to similar data from the nuclear weapon effects literature. In the 1990s, the consensus placed the yield at the low end of this latter range – at 10–15 Mt – partly because of the low probability of a rare large event happening within the last century. According to Brown et al. (2002), only one 10-Mt event should occur per millennium, on average, and a more recent analysis of the rapidly increasing catalog of small asteroids by Alan Harris (personal communication) suggests that the flux of 10-Mt objects is even lower, perhaps by a factor of two. This latter result has led the community to be more willing to accept the low-end estimates (Boslough and Crawford 1997). For this reason, Boslough and Crawford (2008) reexamined the physical basis for why the Tunguska event could have been a 5-Mt or smaller airburst.

Earth and planetary scientists are also beginning to recognize the role that airbursts may have played in geologic history. Tunguska-scale airbursts do not leave any obvious traces in the geologic record. Had Tunguska not been witnessed, it may have never been recognized and studied by the scientific community in later years. Strong and dense asteroids in this size range can reach the ground with more than half of their initial velocity, even while dissipating more than half their kinetic energy into the atmosphere Meteor Crater event can in this sense be classified as a low-altitude airburst, which also included a residual ground impact at reduced velocity, with a fraction of its initial kinetic energy and mass (Melosh and Collins 2005). Airbursts much larger than Tunguska are sufficiently energetic to melt surface materials by radiative heating (Svetsov 2006). Several researchers have suggested that melting and rapid quenching may have left evidence in the form of layered tektites or Libyan Desert Glass (Wasson and Boslough 2000; Wasson 2003) or other fused materials that have not yet been recognized by geologists because they are not associated with impact structures. Putative impact glasses continue to be discovered (e.g., Schultz et al. 2006; Osinski et al. 2006). These glasses may have also been formed by airbursts. Boslough and Crawford (2008) performed numerical simulations intended to provide insight into the phenomenology associated with large low-altitude airbursts.

Airbursts also recently captured the attention those outside the field of impact physics. Firestone et al. (2007) incorporated the concept into an attempt at a cosmic explanation for the Younger Dryas climate change and extinction of North American megafauna about 13,000 years ago. However, their hypothesis was based in part on their misunderstanding of the concept of optimal height of burst and their extrapolation of the Glasstone and Dolan (1977) scaling laws far beyond their range of applicability (limited to altitudes below 100,000 ft). This placed their hypothetical comet explosion at an impossibly high altitude at which it would not be an airburst at all, but an event in outer space. Such an explosion would have required another source of energy. Airbursts rely on atmospheric drag to convert kinetic energy to the

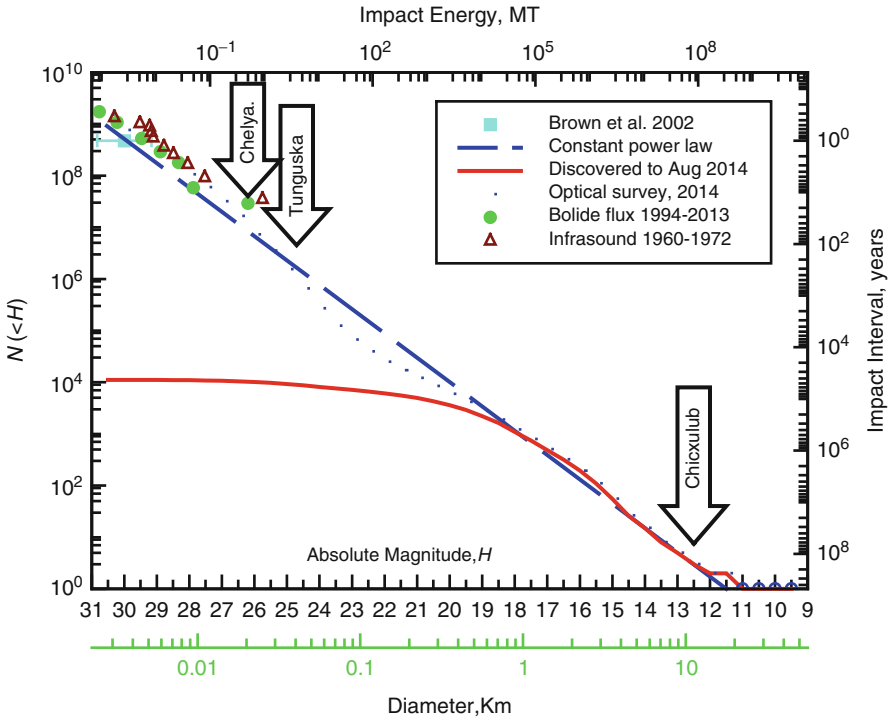

Fig. 1 Near-Earth asteroid population based on optical survey as of 2014 (Alan Harris, personal communication)

thermal energy that is required for an explosion. There are numerous other flaws with the Younger Dryas Impact Hypothesis, summarized by (Boslough et al. 2012).

The following sections show that when a NEO deposits most of its kinetic energy in the lower stratosphere or troposphere, the resulting fireball continues to expand and descend toward the surface, driving a bow shock ahead of it that is reinforced by the explosion. This directed nature of the burst enhances its destructive power relative to a point-source explosion of the same yield at the same altitude (which had been a tacit simplifying assumption for previous risk assessments based on nuclear weapons effects data). According to the latest NEO size distribution plot of Alan Harris (Fig. 1), a Tunguska-class airburst (about 4 Mt) has a mean recurrence interval of about 500 years (with large uncertainty). Earlier estimates of the Tunguska yield were in the 10–20 Mt range, which would also roughly correspond to a 1,000-year event if the size distribution were defined by a constant power law. The latest population estimate from optical surveys for NEOs in the tens-of-meters size range is a significant update. The estimated number of 40-m objects (Tuguska class) has doubled compared to previous estimates.

The fireball resulting from the explosion continues to plow rapidly downward through the atmosphere, driving a shock wave ahead of it as it descends at

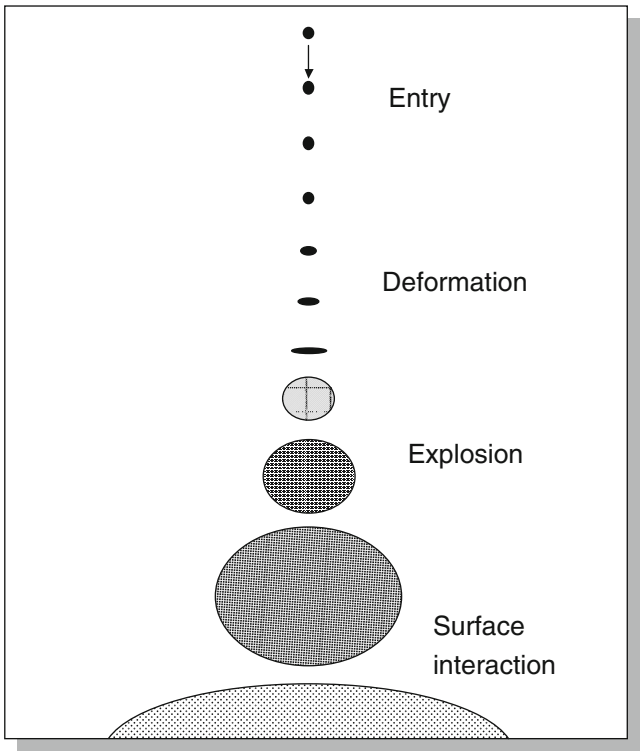

Fig. 2 Schematic diagram of low altitude airburst, showing asteroid (a) entry, (b) deformation (c) explosion, and (d) surface interaction

supersonic velocities. Simulations show that for Tunguska-class events, the fireball stagnates before it reaches the surface and then rises as a buoyant "mushroom cloud." The damage mechanism from Tunguska-type airbursts is dominated by mechanical effects (high wind associated with the blast wave) and thermal radiation. More massive fireballs generated by larger asteroids can descend all the way to the surface and expand radially, leading to incineration of organic material and melting of alluvium and surface rocks. In some simulations, a ring vortex forms, reducing drag forces so that the fireball continues plunging downward. It carries high-temperature air and vaporized meteoritic material to much lower altitude than the simple point-source assumptions would suggest before losing its remaining momentum and beginning to rise due to buoyant forces. Sufficiently large impactors penetrate the atmosphere so deeply before deforming, fragmenting, and exploding that the resultant fireball reaches the surface before losing the remainder of its momentum.

Figure 2 is a schematic diagram of a low-altitude airburst. At (a), the asteroid enters the upper atmosphere and is subjected to aerodynamic drag and ablation. At (b), aerodynamic stress exceeds asteroid strength, deforming it and increasing its

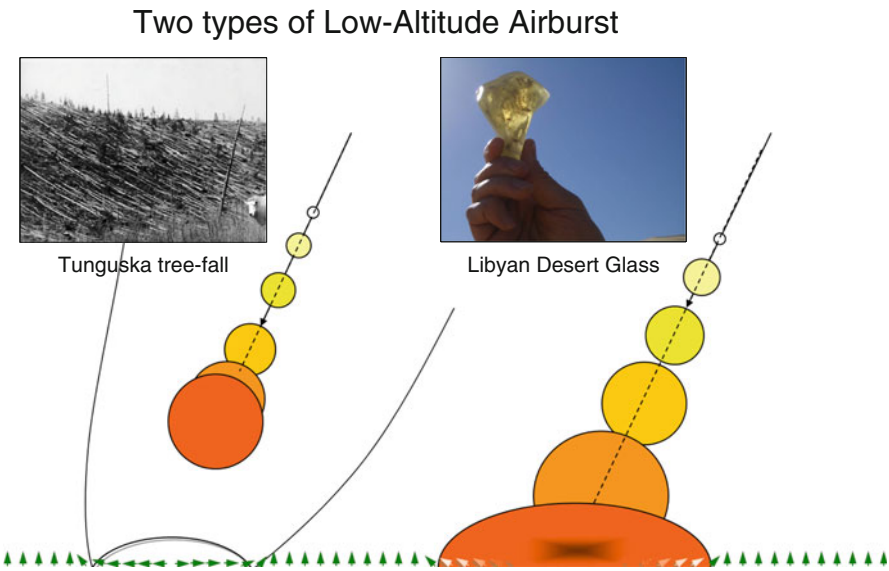

Fig. 3 Left: Type 1 airburst (Tunguska type). Right: Type 2 airburst (Libyan Desert Type)

cross-sectional area. At (c), the asteroid breaks into fragments which rapidly ablate, forming a high-temperature fireball. At (d), the fireball continues to drop to surface where it is held in contact for some period of time by its own inertia. This is consistent with observations of Libyan Desert Glass from an event in the western desert of Egypt 29 Ma ago. These have been defined as two distinct types of airbursts by Boslough (2014), as shown in Fig. 3 where a type 1 airburst (Tunguska type) is shown on the left, and a type 2 airburst (Libyan Desert type) is shown on the right. The following two sections describe the development of models for these two types of airbursts, drawing heavily on the original paper by Boslough and Crawford (2008).

Modeling Type 1 (Tunguska Type) Airbursts

The explosive yield of the Tunguska event has been estimated from observational data and is constrained by nuclear tests, laboratory experiments, and numerical models. Primary observational data include (1) the extent and pattern of fallen trees, (2) seismic records, (3) barograph records, and (4) extent of burned area. The scaling laws of Glasstone and Dolan (1977) provided the principal means for determining the magnitude of a point-source explosion that would be required to generate the observed phenomena. Chyba et al. (1993) used the pancake model described above to constrain the range of impactor size, strength, and kinetic energy based on the physics of atmospheric entry, ablation, deformation, and fragmentation. Taken together, the published evidence all appears to be consistent with a

10–15-Mt event. However, hydrocode simulations have provided the means to discover and examine emergent phenomena – i.e., effects that may not be obvious from first principles considerations – that had not been considered by previous workers. The results of simulations, combined with a reexamination of the surface conditions at Tunguska in 1908, reveal that several assumptions from the earlier analyses have led to erroneous conclusions, resulting in an overestimate of the size of the Tunguska event. Boslough and Crawford (2008) used such simulations to argue that the yield could actually be 5 Mt or lower.

One of the assumptions had been that Tunguska could be treated as a point-source explosion and that nuclear weapons effects provide good calibration. This assumption seemed to have good justification: observations and models of atmospheric entry demonstrate that energy deposition is sharply peaked and concentrated within a scale height of the atmosphere (Chyba et al. 1993). However, the wake of the entry creates a low-density, high-pressure channel from the point of maximum energy all the way out of the atmosphere, so the explosion is highly anisotropic and directed upward and outward (Boslough and Crawford 1997). The resulting high-velocity plume can rise hundreds of kilometers into space for a Tunguska-scale impact much like the plumes that were generated by the impact of fragments of Comet Shoemaker-Levy 9 on Jupiter in 1994. Boslough and Crawford (1997) suggested that such plumes are a hazard to satellites in low Earth orbit.

A second (implicit) assumption has been that downward advection of the explosion can be neglected. In the pancake model, the energy deposition is sharply peaked because of the exponentially reinforcing effects of impactor deformation and atmospheric drag. This peak has been called "airburst height" (Chyba et al. 1993) and is generally considered the altitude at which a point-source explosion of the same yield would have a similar effect on the ground. This assumption neglects the fact that the mass of the projectile is still traveling downward at a significant fraction of its initial speed at the time of its maximum energy loss and can approach or come in contact with the surface as discussed above.

Boslough and Crawford (1997) listed several reasons to be skeptical of estimates that are based on comparisons between the observed damage to the forest at Tunguska and the criteria for blast effects established by the nuclear weapons literature. Yield estimates based on tree fall are too high because they account neither for topography nor forest health. Comparison to nuclear weapon effects is a reasonable approach, but it is important to recognize the limitations associated with using the weapons tables for tree fall, which apply to living coniferous forests and implicitly assume that the surface is flat. Scientific and popular accounts of the Tunguska event state that the forest was flattened over an area of 2,000 km^2. However, old photographs of the destruction show that many trees were left standing. These photographs, as well as contour maps, also reveal that slopes of 15° and greater are typical of the terrain around the impact site (Boslough and Crawford 2008). The topography at Tunguska would naturally lead to concentrations of blast wave energy far beyond the distance that would be calculated

assuming flat terrain, and there appears to be a selection bias in published field photography toward images of the most dramatic locations which are ridges with upslope winds.

Another reason to be skeptical of tree-fall-based yield estimates is that none of them take into account the pre-impact condition of the Siberian forest at the site of the explosion. One result of K.P. Florenskiy's 1961 expedition to the site was that "the region of the forest flattened in 1908 was not one of homogeneous primeval intact taiga" and that ". . .the region of meteorite impact in 1908 was basically a fire-devastated area. . . a partly flattened dead and rotting forest was standing in this area. . .." According to Florenskiy (1963), ". . .an estimate of the force of the shock wave that is based on the number of flattened trees must necessarily take into consideration the condition of the forest at the time." If the requisite wind speeds are reduced to be consistent with Florenskiy's dynamometer measurements, then the necessary point-source yield is reduced to 3.5 Mt (Boslough and Crawford 1997).

Energy estimates based on coupling to seismic and air waves can be grossly in error if naive assumptions are made. The source of seismic waves from Tunguska is estimated to be a vertical point impulse of 7×10^{18} dyn s (Ben-Menahem 1975). Turco et al. (1982) assumed that this entire pulse of momentum had to be attributed as the momentum of the impacting body, leading them to the conclusion that the impactor energy was about 700 Mt. By contrast, Ben-Menahem (1975) arrived at 12.5 Mt by equating the vertical impulse to that from a nuclear explosion (the explosion itself conserves momentum, but the downward directed impulse is coupled to the seismic wave). Momentum multiplication is a well-known effect for crater-forming impacts on a solid surface, given that the ejected material provides a reaction force in addition to the stopping of the projectile (e.g., Lawrence 1990). Momentum enhancement can also be an effect of large impact-produced airbursts, because the ejection of a hypervelocity plume of air into space creates a transient load on the surface that can also couple to seismic waves. Boslough and Crawford (1997) suggested that a 3 Mt plume-forming impact could generate a sufficiently large impulse to generate the seismic signal from Tunguska.

Shoemaker (1983) likewise assumed a point-source explosion approximation to estimate the yield based on inertia-gravity waves in the atmosphere. For Tunguska, the collapsing plume would couple approximately the same momentum back into the atmosphere that the plume originally coupled to seismic waves when it was ejected (but about 10 min later and over a much different time and spatial scale). Boslough and Crawford (1997) also suggested that the bright skies widely observed over Europe and Asia following the Tunguska explosion provides independent evidence for a collapsed plume. Artemieva and Shuvalov (2007) have performed simulations that support this view, but it has not yet gained full acceptance. For example, Bronshten (2000) still prefers the long-standing hypothesis that the bright nights were caused by a comet tail associated with the impact.

The primary motivation for revisiting Tunguska with new simulations is the expectation that significant impact energy is advected downward within the exploding fireball. Boslough and Crawford (2008) solved the pancake model Eqs. 1, 2, and 3

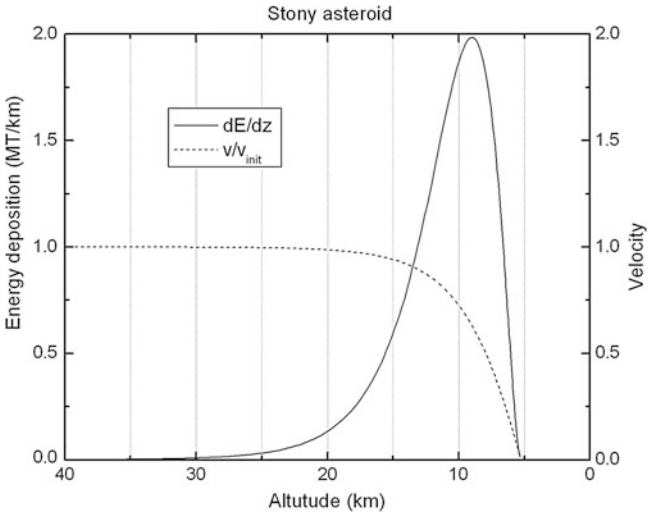

Fig. 4 Energy deposition curve and fractional velocity of 15 Mt stony asteroid based on pancake model

numerically for a stony asteroid using the parameters of Chyba et al. (1992) for the stony asteroid they believe comes closest to consistency with the observations at Tunguska. An initial velocity of 15 km/s, diameter of 58 m, and density of 3.5 g/cm^3, and entry angle of 45° (representing a 15 Mt impact for the right circular cylindrical geometry assumed by the pancake model), yield the energy deposition and velocity curves of Fig. 4. The maximum energy deposition of about 2 Mt/km is reached at an "airburst altitude" of about 9 km above the surface, at which time the exploding asteroid is still descending at a velocity of about 9 km/s (60 % of its initial velocity). Boslough and Crawford (2008) presented a series of Tunguska-scale airburst simulations using the Eulerian shock-physics code CTH. Their primary goal was to explore parameter space in an effort to develop a qualitative understanding, from which new models can be developed that more properly capture the physics. They ran dozens of simulations in which they varied size, impact energy, and material properties (strength and density) over a wide range of values. They used adaptive mesh refinement to sufficiently resolve the entry dynamics while still spanning the entire atmosphere of interest. They also performed simulations using 2-D axial symmetry, which allowed the quick turnaround times needed for scoping and sensitivity analysis. They found phenomena that emerged regardless of the assumptions, over a large range of realistic values. Three representative simulations are shown here. In all these illustrative cases, the asteroid was modeled as a porous dunite sphere that vertically enters the gravitationally stabilized Earth atmosphere. These simulations all used an entry velocity of 20 km/s. Initial masses were adjusted so that initial kinetic energies were 3.0 Mt.

In order to examine the post-airburst hydrodynamics, an additional internal energy was included as a source term that initiated the explosion at a prescribed

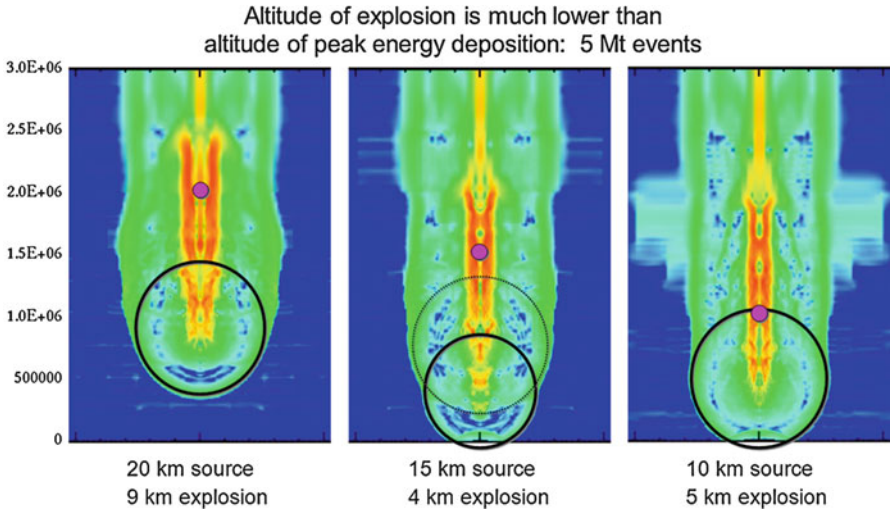

Fig. 5 Three 2D simulations of 5 Mt bursts where asteroid explodes at (a) 20, (b) 15, and (c) 10 km about the surface

altitude. Over the span of several computational time steps, they added 2.0 Mt to the asteroids, bringing the total energy associated with the impacts to 5.0 Mt. The resulting energy density of the asteroid causes it to instantly vaporize, lose strength, and expand as a fireball while maintaining its downward momentum. This provided an extreme case to provide a bound on phenomena associated with rapid fragmentation, ablation, and explosion of the object. The justification for a nearly instantaneous conversion of kinetic to internal energy of the disintegrating body is made by Svetsov (1996), who showed that a Tunguska-scale stony asteroid can be disrupted by the peak aerodynamic load into fragments smaller than 10 cm, which are totally ablated by the high-temperature fireball.

As the fireball descends at hypersonic speed, its translational motion continues to drive a downward bow shock, which is reinforced by its radial expansion. This contrasts with descriptions in much of the Tunguska literature, which describe a "ballistic wave" (the bow shock) and "explosion wave" as being two distinct phenomena (e.g., Zotkin and Tsikulin 1966). In reality, there is only one wave but it obtains its energy from both directed and radial components of kinetic energy. Figure 5 shows snapshots for each of the simulations, a few seconds after the explosion energy was sourced at the specified altitude, where velocity shading is used to enhance visibility of shock wave. Three simulations of 5-Mt bursts are shown, where asteroid explodes at (a) 20, (b) 15, and (c) 10 km about the surface. A magenta dot identifies the locations at which 2.0 Mt of energy was sourced to initiate the explosion. The explosion-reinforced bow shock takes on a spherical shape, which can be used to determine the apparent airburst altitude (as opposed to the altitude where the explosion was initiated). This spherical low-altitude blast wave is centered on apparent airburst altitudes of 9, 4, and 5 km, respectively.

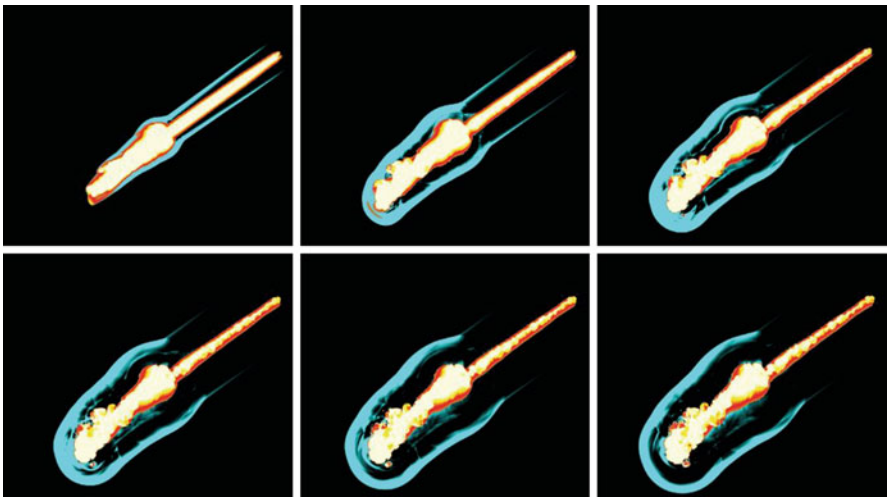

Fig. 6 Cross-sectional snapshots from a 3D simulation of a 5 Mt explosion initiated 12 km above the surface, a good representation of the Tunguska event. Temperature shading (orange to white) represents the wake and fireball, and kinetic energy density (cyan) shading represents the shock wave

In some cases, such as (b), there are multiple apparent burst altitudes. In all cases the height of the apparent airburst is significantly lower than the point of maximum energy deposition. Notably, the fireball penetrates more deeply for the 15 km explosion than for the 10 km explosion.

One unanticipated result is the formation of a large ring vortex, which is initiated by the rapidly descending air mass in some cases. When such a vortex forms, it reduces the aerodynamic drag between the fireball and the surrounding air, allowing the hot mass to reach a lower altitude before stopping. It appears from these preliminary simulations that vortex formation is related to perturbations in the large-scale hydrodynamic flow and may be chaotic in nature. If this is true, then the effects on the ground may strongly depend on the chaotic nature of the fragmentation process that determines the macroscopic flow pattern, adding to the inherent statistical uncertainties in the hazard associated with low-altitude airbursts. These results suggest that the pancake model needs to be modified to include a "post-burst" phase that more properly accounts for the reduced drag on a rapidly expanding, rapidly descending fireball.

Full three-dimensional simulations provide further support for the directed nature of low-altitude airbursts. Figure 6 shows a series of snapshots of a cross-section of a 5-Mt explosion initiated at 12 km above the surface by sourcing 10 % of the internal energy. The fireball is seen to continue descending along its trajectory, driving an asymmetric, explosively reinforced bow shock toward the surface. Figure 7 shows color-coded expanding air shocks on surface maps of two such simulations of a 15-Mt burst (left) and a 5-Mt burst (right). The color bar shows the wind velocity and indicators of forest damage derived from Glasstone and Dolan (1977) with

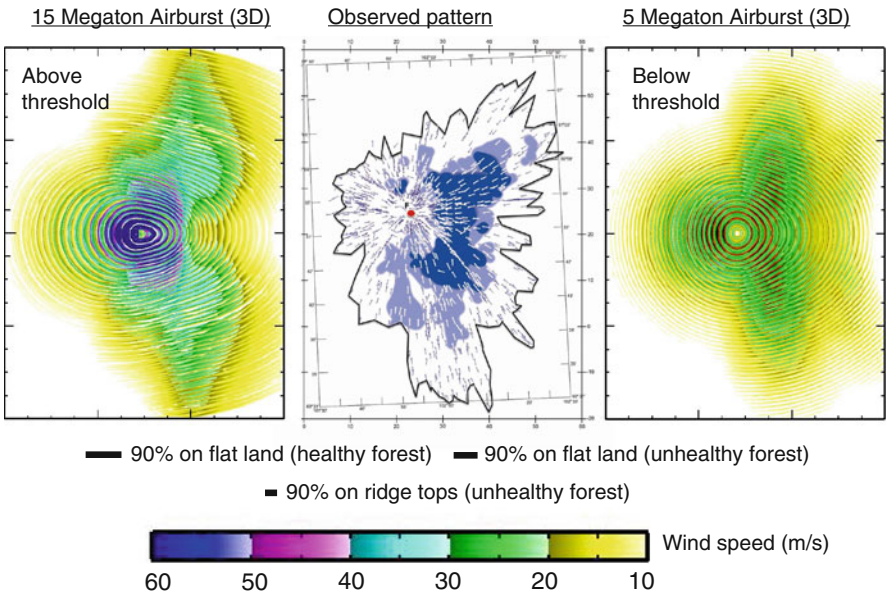

Fig. 7 Simulated 5-Mt airburst (right) provides better match to Tunguska obsrvations (center) than simulated 15-Mt airburst (left)

adjustments for topographic and forest health effects by Boslough (2014). When these model maps are compared to an actual forest damage map of Longo et al. (2005), it can be seen that the damage pattern from the 15 Mt explosion is too extensive, as well as too intense at the epicenter. The 5-Mt explosion provides a much better match.

Modeling Type 2 (Libyan Desert Type) Airbursts

Most natural glasses are volcanic in origin and have chemical compositions consistent with equilibrium fractional melting. The rare exceptions are tektites and glass in melt sheets formed by shock heating associated with the hypervelocity impact of a comet or asteroid. Recent work has explored the possibility that large low-altitude airburst explosions have been responsible for creating deposits of enigmatic glass that appears to be produced by impact but does not seem to be melted by high-pressure shock waves. Unlike most tektites, which exhibit aerodynamic shapes consistent with hypervelocity traversal through the atmosphere, the Muong-Nong tektites of Southeast Asia and the Libyan Desert Glass of western Egypt have a layered structure, suggesting that they experienced laminar flow and sedimentation, and probably formed in place. The chemical composition of these glasses eliminates any possibility of a volcanic origin, and the large areal extents (690,000 km^2 for the Muong-Nong tektites and up to 6,500 km^2 for the Libyan

Desert Glass) have been somewhat of a mystery. If they had formed as a coherent melt sheet by the process of direct shock melting, their area would be limited to the size of the crater in which they formed. Moreover, no impact structure has been found in association with either of these glass deposits, although it is not unreasonable to expect that a crater could be eroded or buried under sediment.

Wasson (2003) considered the possibility of large aerial bursts in the range of 10^{19}–10^{20} J (roughly 10^{3}–10^{4} Mt). One impact of that magnitude takes place every hundred thousand years or so on average. By estimating the amount of energy necessary to provide sufficient heat to the atmosphere, Wasson suggests that the Muong-Nong (layered) tektites would require an impactor energy of 6.5×10^{21} J and all of it would have had to be coupled directly to the atmosphere. Wasson cites constraints on impactor size provided by Ir concentrations in the fallout from this event, concluding that this projectile would have had to be a comet. In Wasson's scenario, a combination of an oblique entry angle and low strength would be necessary conditions for most of the comet's energy to be deposited in the atmosphere. However, observations of Earth-crossing comets suggest that they do not impact the Earth frequently enough to make this plausible for an event that happened less than a million years ago (the age of these tektites is only 0.78 Ma). Only three comets cross Earth's orbit every year, on average, most of which are in the 1- to 2-km diameter range required by Wasson. This flux is consistent with an impact frequency of only one per 150 Ma. A low-probability oblique impact reduces the likelihood of such an event even further, virtually eliminating it as a plausible explanation.

Wasson's assumption, however, was that the atmosphere would have to be heated from top to bottom over a significant fraction the entire area of the melt sheet to a temperature of 2,500 K. However, if the surface material was melted from radiated energy, there would be no need for the atmosphere to be at high temperature over the entire area simultaneously. When the high-temperature fireball produced by a low-altitude airburst expands, it temporarily displaces the colder, higher-density atmosphere. Moreover, the most common elevation angle for an asteroid impact is 45°, and airburst simulations suggest that the fireball will retain a significant fraction of the initial momentum of the asteroid (perhaps in a low-drag configuration enhanced by a ring vortex). In this way, the expanding fireball can move horizontally for a long distance, passing over and heating an area many times larger than itself. Perhaps a better estimate of the magnitude of the required yield would be from the mass of the glass itself. Wasson estimated the mean thickness of the sheet to be about 4 mm, with a total mass of about 10^{16} g, which would require the influx of roughly 10^{19} J to heat and completely melt. A chondritic asteroid with a mass of 1.5×10^{15} g is consistent with the Ir concentrations (Schmidt et al. 1993). The impact frequency for asteroids of this size is about one per million years, so the likelihood of an oblique impact at 0.78 Ma is reasonable. An asteroid of that size impacting at 20 km/s would only need to transfer 3 % of its kinetic energy through the atmosphere into the ground as heat to melt the requisite volume. Significantly, such a small fraction of energy required for coupling to the atmosphere does not eliminate the possibility of a crater-forming event that was accompanied by an airburst.

Fig. 8 Clear and frothy specifmen of Libyan Desert Glass

The 29 million-year-old Libyan Desert Glass (LDG) represents another candidate material that may have formed by radiative melting from a low-altitude airburst. Unlike the SE Asian tektites, LDG fragments have probably been transported laterally over long distances since they were formed, so it is not necessary to invoke a hot atmosphere that spans the entire area in which they are found. The LDG is composed of 98 % SiO_2 and has a composition similar to that of the sandstone bedrock and dune sands of the Great Sand Sea where it is located. The physical structure of the glass fragments provide clues to how it was formed and do not appear to be consistent with either shock melting at high pressure or hypervelocity traversal of the atmosphere. Some fragments are yellow-green and highly transparent with embedded bubbles that are highly elongated along an apparent flow axis, while others are opaque and white, giving the appearance of foam (Fig. 8). Microscopic examination of the white glass reveals dense spherical bubbles about 100 μm in diameter, suggesting that air was injected during frothy, turbulent flow of a very low-viscosity liquid. Many pieces show streaks of darker material, often aligned in the apparent flow direction. Koeberl (2000) has shown that at least some of this darker material has a meteoritic component.

There is no known impact structure in the immediate vicinity of the LDG. However, Kleinmann et al. (2001) have shown that local sandstones have been strongly shocked, so there is unambiguous evidence for a solid crater-forming impact. The question is whether the surface impact represented a significant fraction of the energy deposition and if it had anything to do with glass formation. To help answer this question, Boslough and Crawford (2008) performed CTH simulations of the atmospheric entry of a 120-m-diameter sphere of dunite. With an initial velocity of 20 km/s, the asteroid had a kinetic energy of about 108 Mt. Even at vertical incidence, most of the energy is coupled directly into the atmosphere as the asteroid ablates and explodes before it hits the ground. In this case, the resulting fireball (which contains air and ablated meteoritic material at temperatures

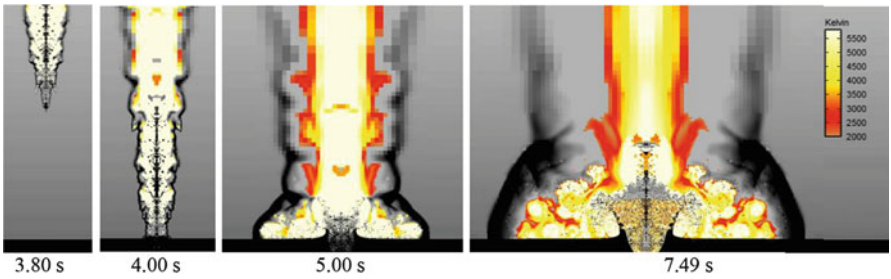

Fig. 9 Snapshots from 2D simulation of Type 2 airburst that may represent Libyan Desert Glass event. Fireball is shaded by temperatures ranging from red (2000 K, the approximate melting temperature of silica) and white (5800 K, the approximate surface temperature of the sun). Air density is shaded gray, showing shock wave

exceeding the melting temperature of quartz) makes direct contact with the surface over a 10-km-diameter area for more than 10 s after the explosion. Figure 9 shows the simulation of a low-altitude airburst for which the fireball descends to the surface. In the figure, white represents 5,800 K (the approximate surface temperature of the sun) and red represents 2,000 K (the approximate melting temperature of quartz). At the interface between the fireball the surface, wind velocities exceed the sound speed for tens of seconds.

The results of this simulation seem to provide answers to two oft-cited objections to the airburst hypothesis for LDG. First is the question of how bubbles of significant size could have escaped a viscous fluid (LDG is nearly pure silica, which is remains highly viscous at elevated temperature). Friedman and Parker (1969) measured the high-temperature viscosity of LDG and calculated that bubble removal would require a temperature of 1,600 °C for 47 days, 1,800 °C for 0.5 day, or 2,000 °C for 2 min. They preferred an explanation that invoked a very high temperature for a very short time. Since the postshock temperatures in silica can achieve these high levels for a hypervelocity impact (e.g., Boslough 1988) the preferred explanation has remained with direct shock melting. However, direct exposure to a 5,000 K fireball would raise the temperature of the melt beyond those considered by Friedman and Parker (1969), further lowering its viscosity and easing the constraint on time required. The second objection is that the observed sizes of LDG fragments (>10 cm) greatly exceed the thickness of silica that could be heated by a 10-s pulse of radiation. A simple diffusion calculation suggests that a layer of only a few mm could be heated above the silicate melting temperature (e.g., Svetsov 2006). However, this calculation neglects the fact that in a low-altitude airburst, the surface materials will be subjected to supersonic winds at the same time as the thermal pulse and any melt layer will be ablated. Repeating the diffusion calculation, discarding any material above the melt temperature and re-applying a flux condition to the new boundary suggests that several cm can be ablated. It is reasonable to expect that melt would blow downrange where it would collect in pools and form glass with larger dimensions.

Modeling the Chelyabinsk Event

The previous examples of models apply to one poorly observed historical event (Tunguska) and one unobserved prehistoric event (the LDG event). Until Feb. 15, 2013, no high-quality real-time data had ever been collected on a megaton-scale airburst. In the early-morning hours of that day, a small asteroid exploded over a rural area about 40 km south of the Russian city of Chelyabinsk. Its proximity to a population center led to many injuries and widespread blast damage but also yielded a plethora of serendipitous data in the form of video footage from security and dashboard cameras. Combined with seismic, infrasound, satellite records, and meteorite studies, this data provides a rich and multifaceted means to determine the projectile size and entry parameters and to develop a self-consistent model and understanding of the airburst (Brown et al. 2013; Borovička et al. 2013; Popova et al. 2013; Kring and Boslough 2014).

The best estimate of the kinetic yield (explosive energy) is 400–500 kt (Brown et al. 2013), making Chelyabinsk the most powerful such event observed since Tunguska. Analysis of videos combined with subsequent on-site stellar calibrations have enabled precise estimates of entry velocity (19 km/s), angle (17° from the horizontal) and altitude of peak brightness (29 km) (Borovička et al. 2013). This implies a pre-entry diameter of ~20 m and mass of ~12,000 tones. Satellite sensors recorded the emission peak at 03:20:33 UT, with a total radiated energy of 3.75×10^{14} J (~90 kt). A typical bolide luminous efficiency of 20 % implies a total yield of about 450 kt, consistent with infrasound and other observations. The maximum radiant intensity was 2.7×10^{13} W/ster, corresponding to a magnitude of −28.

The shallow entry angle led to a very long duration of the bolide (16.5 s) and energy was deposited over hundreds of km, leading to an extended, near-horizontal, and high-altitude linear explosion. The blast wave was distributed over a large area, and because of divergence, it was much weaker than it would have been for a steep entry and a more concentrated explosion closer to the surface. The orientation also led to different phenomena than expected for a more vertical entry. There was no ballistic plume as observed from Shoemaker-Levy 9 impacts on Jupiter (45°) and calculated for Tunguska (~35°). Instead, buoyant instabilities grew into mushroom clouds and the trail bifurcated into two contrarotating vortices.

Information gained from observational data to initialize hydrodynamic simulations with extremely accurate energy depositions at well-defined locations has now been used to initialize computational simulations. Results can be compared to observations (such as timing and distribution of blast energy at the surface and evolution of the trail). This will lead to better validation of the models and understanding of the physical phenomena associated with airbursts.

Analysis is still in the early stages and detailed model results have not yet been published. Figure 10 shows two snapshots of the cross section of a preliminary 3D simulation, in which instabilities along the wake can be seen to form, as well as the early stages of mushroom clouds. Because of the shallow entry angle, the momentum carries the fireball sideways and only slightly downward after the explosion. The energy is therefore spread out over a larger area but is less damaging on the

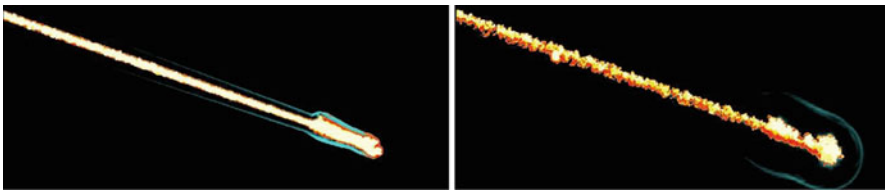

Fig. 10 Snapshots from a preliminary 3D simulation of the Chelyabinsk airburst

surface than it would have been if it had entered at a steeper angle. Figure 11 shows a cross section of a preliminary 2D simulation that is perpendicular to the wake. This illustrates the mechanism for the formation of two trails due to the bifurcation of the cylindrical hot wake as it rises buoyantly, generating two contrarotating linear vortices in which ablated asteroid material condenses into clouds. Detailed quantitative models of this effect have not yet been developed

According to new optically based size/frequency curves shown in Fig. 1, Chelyabinsk is approximately a 50-year event and Tunguska is a 500-year event. These two events suggested that the previous optically-based population had underestimated the frequency of large airbursts. The updated population shown in Fig. 1 brings them into closer agreement. Since models also show that they are more damaging than nuclear explosions of the same magnitude (traditionally used to estimate impact risk), the risk from airbursts is likely greater than previously thought. The next section gives an example of how modeling can assist plans to mitigate the hazard of airbursts.

Modeling Airbursts for Disaster Planning

One significant finding of the NRC report *Defending Planet Earth* (2010) was that "it is highly probable that the next destructive NEO event will be an airburst from a <50-m object, not a crater-forming impact." The associated recommendation was

> Because recent studies of meteor airbursts have suggested that near-Earth objects as small as 30 to 50 meters in diameter could be highly destructive, surveys should attempt to detect as many 30- to 50-meter objects as possible. This search for smaller-diameter objects should not be allowed to interfere with the survey for objects 140-meters in diameter or greater.

It is reasonable to transition surveys toward short-warning objects on their "death plunge" into Earth's atmosphere. If an object is found within a few days of impact, lives could be saved through civil defense.

One option for responding to short-warning airburst objects would be analogous to the National Hurricane Center, which provides regularly updated information to authorities who are responsible for evacuation or shelter orders. Like hurricanes, there would be many uncertainties associated with short-warning objects, but the nature of the uncertainties would be very different. The trajectory and impact

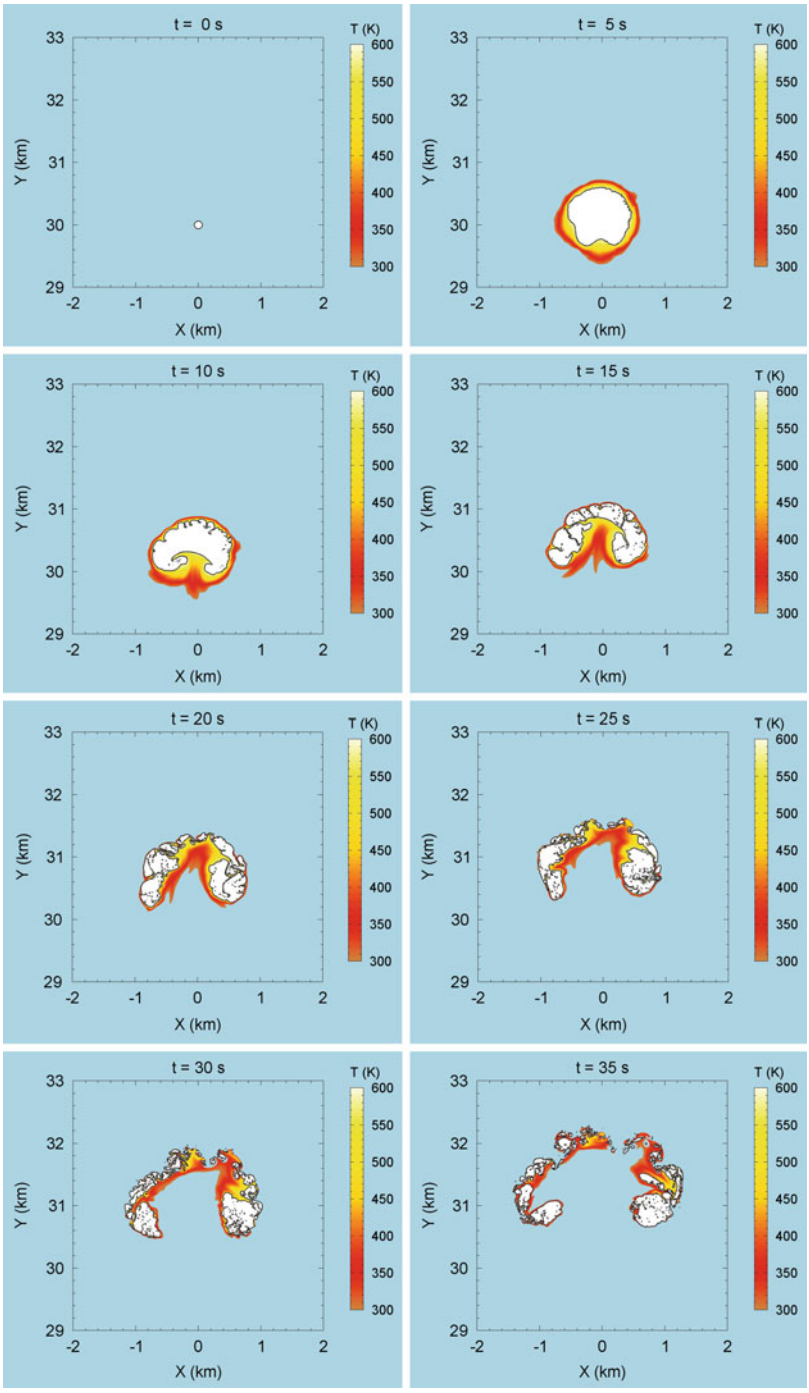

Fig. 11 (continued)

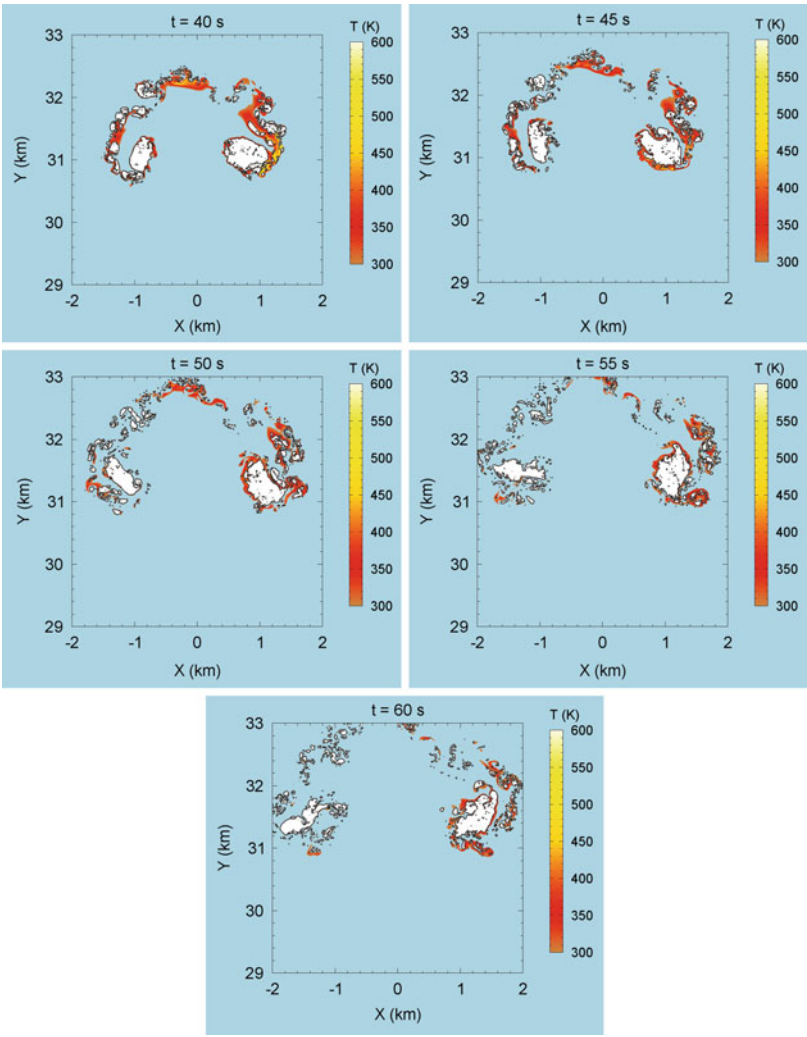

Fig. 11 Snapshots of 2D simulation showing evolution of cross-section of Chelyabinsk wake where temperatures range from several hundred degrees K (red) to a few thousand degrees K (yellow)

location uncertainty would diminish very quickly as the NEO is tracked, but the mass, strength, density, and other material properties that control burst altitude and destructive potential would remain uncertain and any civil defense measure would need to take this uncertainty into account.

To plan for such an event, a tabletop exercise (TTX) was held at FEMA headquarters on May 20, 2013, at the request of NASA's Near-Earth Objects Program Office. The exercise consisted of the scripted discovery, tracking, and characterization of an asteroid, mission planning and mitigation response, and

explicit quantification of uncertainty associated with the evolution of knowledge about the threat. Information collected during the exercise is now being used to help guide a detailed study of short-warning threats. Participants at the meeting included representatives of NASA, Department of Defense, Department of State, Department of Homeland Security/Federal Emergency Management Agency (FEMA), and the White House. The cover letter sent to participants read as follows:

> The President has activated the ESFLG [Emergency Support Function Leadership Group] to prepare for an immanent and certain disaster that will affect Texas and neighboring states, as well as states and possibly nations bordering the Gulf of Mexico. The disaster will occur at approximately noon local time on September 5, 2021 and will be caused by impact of an asteroid estimated to be about 50 meters (~160 ft) in diameter. Details of what is currently known about the threat and of our past efforts to deflect the object are included in this package. This disaster will be unprecedented in recorded times and will seriously affect our nation's oil refining and other mayor industries, as well as the lives and property of many of our citizens. Please develop plans to minimize these effects.

To assist in development of the impact scenario, hydrodynamic airburst simulations were used to generate physical effects maps over a range of assumptions, producing maps that could be loaded into an application that resulted in estimates of infrastructure damage over the affected area.

The threat scenario was primarily developed by NASA/JPL. It involved an asteroid in an orbit that is somewhat similar to that of the 2013 Chelyabinsk object. The discovered asteroid was an order of magnitude more massive and was discovered years in advance, rather than not at all. The scenario involved a partially successful deflection attempt that resulted in the impact of a 50-m-diameter fragment (a small fraction of the original mass). It was intended to be an accurate representation of how an asteroid threat might evolve, although each threat would be unique in its evolution. At the current time, because of the lack of comprehensive surveys, an impact of the type could occur with little or no warning.

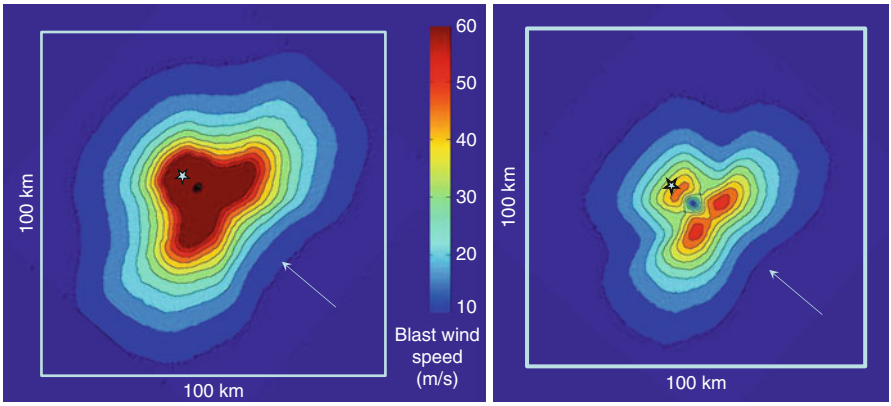

Fig. 12 Contour maps of maximum surface wind speed (in m/s) at directly beneath an airburst from 4.15 Mt explosion (left) and 10.63 Mt explosion (right). In both cases the asteroid descends at 40 degrees from the horizontal and explodes at 12 km

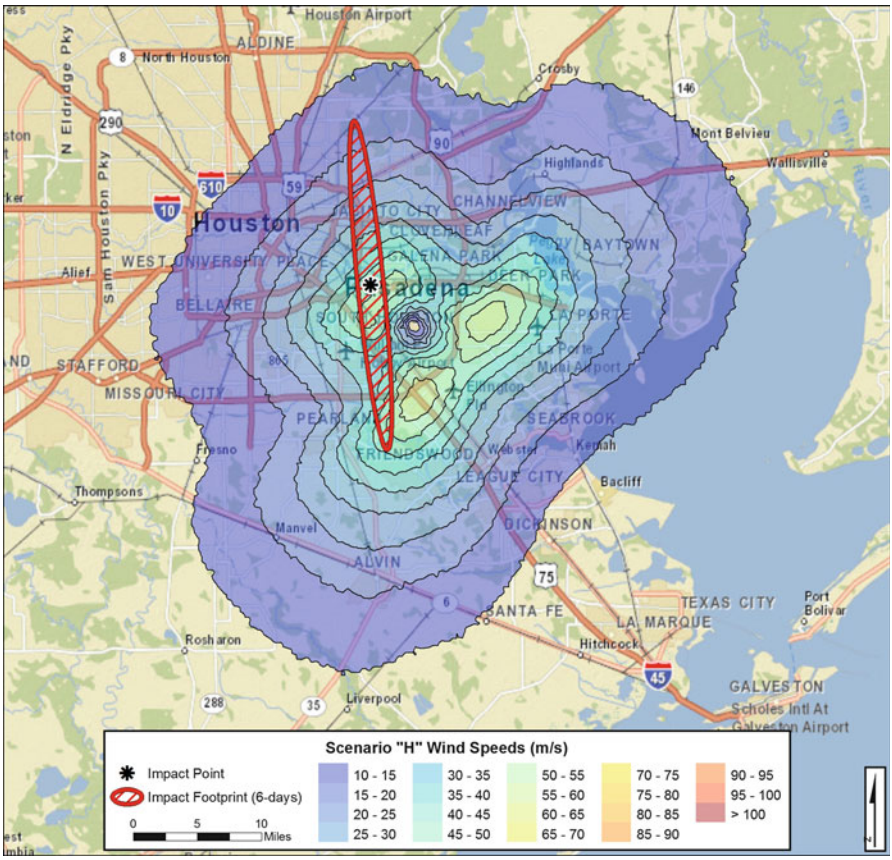

Fig. 13 CTH-generated wind speed contours from a 4.15 Mt airburst over Houston from a 50-m asteroid superimposed on map with impact uncertainty ellipse

The resulting impact would be expected to yield an airburst very similar to the explosion over the Tunguska region of Siberia in 1908. One widely accepted estimate of the equivalent explosive yield of Tunguska is 3–5 Mt with an entry angle of 35° above the horizon, whereas the simulated best estimate of the TTX impact was 4.15 Mt with an entry angle of 40°. To be realistic, the exercise assumed that the exact diameter of the impacting object would still be somewhat uncertain immediately prior to the event. The density (thus the mass and yield) and the strength (thus the burst altitude) would be highly uncertain. Therefore, the approach was to perform a matrix of simulations using CTH over a wide range of assumptions that included the best estimate as well as the worst case.

For purposes of the TTX, the damage was assumed to be dominated by dynamic pressure associated with the blast wave at the surface beneath the burst. When an asteroid deposits most of its kinetic energy in the lower stratosphere or troposphere, the resulting fireball continues to expand and descend toward the surface, driving a

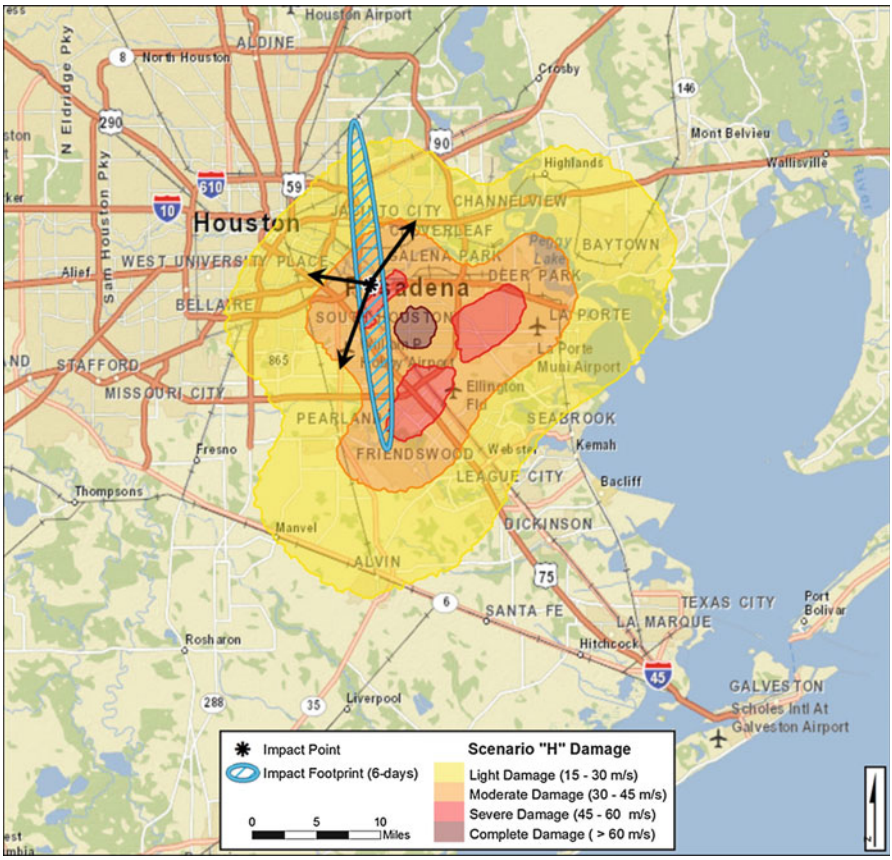

Fig. 14 Damage contours for airburst shown in Fig. 13. Arrows indicate evacuation plan if there were no uncertainty in impact point

bow shock ahead of it that is reinforced by the explosion. As discussed above, this directed nature of the burst enhances its destructive power relative to a point-source explosion of the same yield at the same altitude (which had been a tacit simplifying assumption for previous risk assessments based on nuclear weapons effects data. Small crater-forming impacts are also accompanied by such airbursts.

Exploding asteroids of various sizes, densities, and prescribed burst altitudes in a gravitationally stabilized atmosphere were simulated, allowing the blast wave to propagate to a radial distance of 50 km on the surface. These simulations yielded contour maps such as those shown in Figure 12. In all cases the asteroid was exploded at the prescribed altitude by sourcing additional energy to cause it to vaporize. For these simulations 10 % of the original kinetic energy was used and the impact velocity was reduced to compensate to keep the total energy at the correct value. This effectively underestimates the momentum by a few percent, so the coupling to the ground is a slight underestimate. Two examples of contour plots of

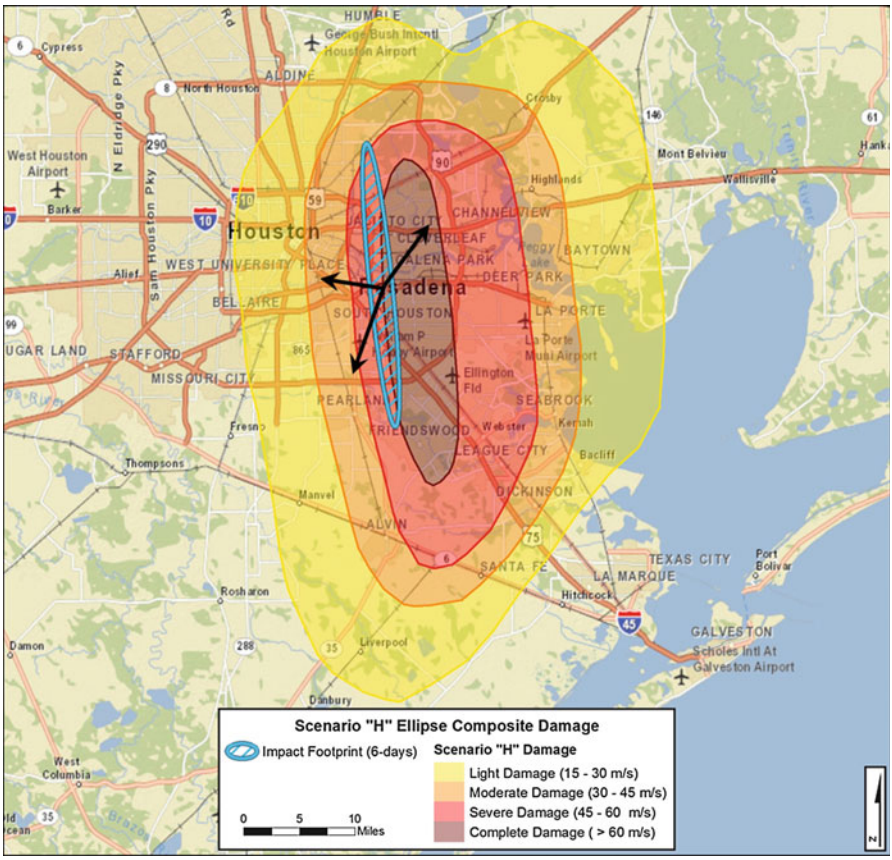

Fig. 15 Worst-case damage contours for Fig. 13 airburst due to uncertainty in impact point

maximum wind speeds from airburst simulations are shown: left, best estimate (50 m, 2.2 g/cm^3, burst altitude 12 km, 4.15 Mt), and right, worst case (60 m, 3.3 g/cm^3, burst altitude 12 km, 10.6 Mt). Velocity is in cm/s. Graphs are 100 km squares. Ground track is from lower right to upper left.

Figure 13 shows the best estimate projected onto geospatial coordinate system, where the projected impact point is within the notional error ellipse 6 days before impact. In Fig. 14, the horizontal wind speeds were transformed into assumed infrastructure damage estimates (accounting for other damage mechanisms such as vertical winds and overpressure that dominates at the epicenter). Figure 15 shows a convolution of the damage map for a known impact point with the uncertainty ellipse, yielding a map of domains that define the worst possible damage that can be expected at various locations. It is important to note that not all locations within a domain will suffer the maximum damage, but these maps explicitly account for uncertainty in impact location.

These figures together illustrate potential evacuation issues associated with uncertainty. Figure 14 illustrates a hypothetical situation in which perfect knowledge is available, with a calculated damage map and the most efficient evacuation routes. Figure 15 shows that by including uncertainty, potentially inappropriate evacuation instructions can be eliminated.

Conclusion

Computational modeling is a powerful method for gaining insight into the physics of airbursts, as well as for generating quantitative estimates of the degree of the damage they cause. Hydrodynamic code simulations have identified emergent phenomena – including downward-directed ring vortices and upward-directed atmospheric plumes – that must be included in assessments of the impact hazard and the evidence in the geologic record. Semi-analytical airburst models can be extended to account for ring vortex formation, buoyant forces, and surface interactions of the fireball, from which better estimates of air blast and radiative damage zones can be made over the range of possible airburst scenarios. Comparing simulated damage maps to the actual data should provide much tighter and more convincing constraints on the low-altitude airburst at Tunguska. Quantitative risk assessments can be generated by combining these simulations with impact probability density functions from known astronomically-determined size distributions, thereby informing policy decisions.

Since airbursts are statistically the most frequent impact events that can have an effect on the ground, the next impact on Earth that causes casualties or property damage will almost certainly be another low-altitude airburst. Downwardly directed airbursts are more damaging than nuclear weapons of the same yield, because they are not point sources. To date, airburst modeling at Sandia National Laboratories has been limited to a small set of cases in which many assumptions had to be made: the 1994 impact of Comet Shoemaker-Levy 9 on Jupiter, the 1908 Tunguska event, the 29 Ma glass-forming Libyan Desert event, the 2013 Chelyabinsk event, and a hypothetical airburst over Houston for a 2014 FEMA tabletop exercise. The primary purpose of airburst simulations thus far is to gain insight about the phenomenon and to develop methods. Computational tools now exist to perform a large matrix of simulations over a large range of parameters including size, velocity, burst altitude, and entry angle; to generate damage maps on the ground for a given location; and to estimate the loss of infrastructure and economic costs. Fidelity can be further improved by extending to a wider range of scales (including smaller dimensions that resolve the breakup process itself) and by using versions of existing hydrocodes that include more physics, such as radiation transfer.

Acknowledgments Sandia National Laboratories is a multiprogram laboratory managed and operated by Sandia Corporation, a wholly owned subsidiary of Lockheed Martin Corporation, for the US Department of Energy's National Nuclear Security Administration under contract DE-AC04-94AL85000. This work was funded by Sandia's LDRD program and by NASA.

Cross-References

- European Operational Initiative on NEO Hazard Monitoring
- Minor Planet Center
- Space-Based Infrared Discovery and Characterization of Minor Planets with NEOWISE
- Water Impact Modelling

References

Artemieva N, Shuvalov V (2007) 3D effects of Tunguska event on the ground and in atmosphere (abstract). Lunar and planetary science XXXVIII. Lunar and Planetary Institute, Houston

Ben-Menahem A (1975) Source parameters of the Siberian explosion of June 30, 1908, from analysis and synthesis of seismic signals at four stations. Phys Earth Planet Inter 11(1):1–35

Borovička J et al (2013) The trajectory, structure and origin of the Chelyabinsk asteroidal impactor. Nature 503:235

Boslough MB (1988) Postshock temperatures in silica. J Geophys Res 93:6477–6484

Boslough M, Nicoll K, Holliday V, Daulton TL, Meltzer D, Pinter N, Scott AC, Surovell T, Claeys P, Gill J, Paquay F, Marlon J, Bartlein P, Whitlock C, Grayson D, Jull AJT (2012) Arguments and Evidence Against a Younger Dryas Impact Event, in Climates, Landscapes, and Civilizations. In: Giosan L, Fuller DQ, Nicoll K, Flad RK, Clift PD (eds), American Geophysical Union, Washington, DC. doi: 10.1029/2012GM001209

Boslough M (2014) Airburst warning and response. Acta Astronautica 103:370–375. DOI: 10.1016/j.actaastro.2013.09.007

Boslough MBE, Crawford DA (1997) Shoemaker-Levy 9 and plume-forming collisions on Earth (near-earth objects). Annals NY Acad Sci 822:236–282

Boslough M, Crawford D (2008) Low-altitude airbursts and the impact threat. Int J Impact Eng 35:1441–1448

Bronshten VA (2000) Nature and destruction of Tunguska cosmical body. Planet Space Sci 48(9):855–870

Brown P, Spalding RE, ReVelle DO, Tagliaferri E, Worden SP (2002) The flux of small near-Earth objects colliding with the Earth. Nature 420:294–296

Brown P et al (2013) A 500-kiloton airburst over Chelyabinsk and an enhanced hazard from small impactors. Nature 503:238–241

Chyba CF, Thomas PJ, Zahnle KJ (1993) The 1908 Tunguska explosion: atmospheric disruption of a stony asteroid. Nature 361:40–44

Firestone RB et al (2007) Evidence for an extraterrestrial impact 12,900 years ago that contributed to the megafaunal extinctions and the Younger Dryas cooling. Proc Natl Acad Sci USA 104:16,016–16,021

Florenskiy KP (1963) Preliminary results from the 1961 combined Tunguska meteorite expedition. Meteortica XXIII:3–37

Friedman I, Parker CJ (1969) Libyan desert glass: its viscosity and some comments on its origin. J Geophys Res 74:6777–6779

Glasstone S, Dolan (1977) The effects of nuclear weapons. U.S. Dept. of Defense/Dept. of Energy, Washington DC, 653 pp http://www.deepspace.ucsb.edu/wp-content/uploads/2013/01/Effects-of-Nuclear-Weapons-1977-3rd-edition-complete.pdf

Kleinmann B, Horn P, Langenhorst F (2001) Evidence for shock metamorphism in sandstones from the Libyan Desert Glass strewn field. Meteor Planet Sci 36:1277–1282

Koeberl C (2000) Confirmation of a meteoritic component in Libyan Desert Glass from osmium isotope data (abstract). In: 63rd annual meteoritical society meeting

Kring DA, Boslough M (2014) Chelyabinsk impact airburst. Physics Today, Sept 2014
Lawrence RJ (1990) Enhanced momentum transfer from hypervelocity particle impacts. Int J Impact Eng 10:337–349
Longo G, Di Martino M, Andreev G, Anfinogenov J, Budaeva L, Kovrigin E (2005) A new unified catalogue and a new map of the 1908 tree fall in the site of the Tunguska Cosmic Body explosion. In: Asteroid-comet Hazard-2005. Institute of Applied Astronomy of the Russian Academy of Sciences, St. Petersburg, pp 222–225
Melosh HJ, Collins GS (2005) Meteor crater formed by a low-velocity impact. Nature 434:157
NRC Committee to Review Near-Earth Object Surveys and Hazard Mitigation Strategies; National Research Council (2010) Defending planet Earth: near-Earth object surveys and hazard mitigation strategies, 152 pp
Osinski GR, Schwarcz HP, Smith JR, Kleindienst MR, Haldemann AFC, Churcher CS (2006) Evidence for a ~200–100 ka meteorite impact in the Western Desert of Egypt. Earth Planet Sci Lett 253(3/4):378–388
Popova OP et al (2013) Chelyabinsk airburst, damage assessment, meteorite recovery, and characterization. Science 342:1069
Schmidt G, Zhou L, Wasson JT (1993) Iridium anomaly associated with the Australasian tektite-producing impact: masses of the impactor and of the Australasian tektites. Geochim Cosmochim Acta 57:4851–4859
Schultz PH (1992) Atmospheric effects on ejecta emplacement. J Geophys Res 97:11623–11662
Schultz PH, Zárate M, Hames WE, Harris RS, Bunch TE, Koeberl C, Renne P, Wittke J (2006) The record of Miocene impacts in the Argentine Pampas. Meteoritics 41(5):749–771
Shoemaker EM (1983) Asteroid and comet bombardment of the Earth. Ann Rev Earth Planet Sci 11:461–494
Svetsov VV (1996) Total ablation of the debris from the 1908 Tunguska explosion. Nature 383:697–699
Svetsov VV (2006) Thermal radiation on the ground from large aerial bursts caused by Tunguska-like impacts (abstract). In: Lunar and planetary science XXXVII. Lunar and Planetary Institute, Houston
Turco RP, Toon OB, Park C, Whitten RC, Pollack JB, Noerdlinger P (1982) An analysis of the physical, chemical, optical, and historical impacts of the 1908 Tunguska meteor fall. Icarus 50:1–52
Vasilyev NV (1998) The Tunguska meteorite problem today. Planet Space Sci 46(2/3):129–150
Wasson JT (2003) Large aerial bursts; an important class of terrestrial accretionary events. Astrobiology 3(1):163–179
Wasson JT, Boslough MBE (2000) Large aerial bursts; an important class of terrestrial accretionary events (abstract). In: LPI Contribution 1053: catastrophic events and mass extinctions: impacts and beyond. Lunar and Planetary Institute, Houston, pp 239–240
Zahnle KJ (1992) Airburst origin of dark shadows on Venus. J Geophys Res 97(E6):10,243–10,255
Zotkin IT, Tsikulin MA (1966) Simulations of the explosion of the Tungus meteorite. Sov Phys Dokl 11:183